Proceedings of the Summer Heat Transfer Conference
SHTC2019
July 15-18, 2019, Bellevue, Washington

HT2019-3425

ELECTROWETTING-BASED COALESCENCE OF DROPLETS DURING DROPWISE CONDENSATION OF HUMID AIR

Enakshi Wikramanayake
Walker Department of Mechanical Engineering
The University of Texas at Austin
Austin, Texas, USA

Vaibhav Bahadur*
Walker Department of Mechanical Engineering
The University of Texas at Austin
Austin, Texas, USA

ABSTRACT

Dropwise condensation yields higher heat transfer coefficients by avoiding the thermal resistance of the condensate film, seen during filmwise condensation. This work explores further enhancement of dropwise condensation heat transfer through the use of electrowetting to achieve faster droplet growth via coalescence of the condensed droplets. Electrowetting is a well understood microfluidic technique to actuate and control droplets. This work shows that AC electric fields can significantly enhance droplet growth dynamics. This enhancement is a result of coalescence triggered by various types of droplet motion (translation of droplets, oscillations of three phase line), which in turn depends on the frequency of the applied AC waveform. The applied electric field modifies droplet condensation patterns as well as the roll-off dynamics on the surface. Experiments are conducted to study early-stage droplet growth dynamics, as well as steady state condensation rates under the influence of electric fields. It is noted that this study deals with condensation of humid air, and not pure steam. Results show that increasing the voltage magnitude and frequency increases droplet growth rate and overall condensation rate. Overall, this study reports more than a 30 % enhancement in condensation rate resulting from the applied electric field, which highlights the potential of this concept for condensation heat transfer enhancement.

NOMENCLATURE

$C_{p,wv}$	Specific heat capacity or water vapor, *kJ/kg*
g	Gravitational acceleration, *m/s²*
Gr	Grashof number
h_{air}	Natural convection heat transfer coefficient, W/m^2.K
h_{fg}	Latent heat of condensation, *kJ/kg*
$\dot{m}''$	Water harvest rate, *kg/m²s*
Q''	Heat flux, *W/m²*
r	Radius, *m*
<R>	Area averaged radius, *m*
$T_{dew\ point}$	Dew point temperature, *°C*
T_s	Surface temperature, *°C*
T_∞	Ambient temperature, *°C*
β	Volumetric thermal expansion coefficient, *1/K*
ν	Kinematic viscosity, *m²/s*

*Corresponding author: vb@austin.utexas.edu

INTRODUCTION

Condensation is important in many applications such as water harvesting [1,2], desalination [3] and electricity generation in power plants [4]. The condensation rate and heat transfer is severely restricted [5] in most applications by the formation of a condensate film on the surface. Heat transfer can be significantly enhanced if water can be made to condense as droplets which then roll-off. This dropwise mode of condensation is observed on hydrophobic and superhydrophobic surfaces. Elimination of the thermal resistance of the water film yields 5-10X higher heat transfer coefficients [6] in dropwise condensation (DWC) when compared to filmwise condensation (FWC). Condensed water droplets roll-off (before merging to form a film) on superhydrophobic surfaces, and expose the surface to fresh vapor for more nucleation.

Many studies have involved the assessment of surfaces which promote dropwise condensation [6–8]. Condensation dynamics and droplet size distributions have been visualized and studied on surfaces with a variety of textures and chemistry [5,7,9,10]. A majority of these studies involved condensation of pure steam; there exist fewer detailed studies on condensation in the presence of non-condensable gases (NCGs) [10,11].

The use of an electric field to promote condensation heat transfer has generated significant recent interest [12–14]. Miljkovic et al. [15] used an electric field to prevent droplets jumping from the surface (due to the energy released via coalescence) from returning back. This improvement leads to a 50 % enhancement in heat transfer. There also exist limited studies on the use of an electric field [16–20] to alter the surface tension of the condensing liquid, and as a tool for enhancing dropwise condensation. Electrowetting (EW) is a well-studied [21,22] fluid handling technique to control the wettability of droplets. EW relies on the application of an electric field across a dielectric layer underlying the droplet, to modulate wettability and also move the droplet. In a recent study, Baratian et al [16] studied the coalescence of droplets condensing from nearly pure water vapor under the influence of a 1 kHz AC EW field. Energy-minimization considerations were used to study condensation patterns and droplet size distributions. Another study from the same group showed that certain EW configurations can reduce droplet shedding radii and achieve faster roll-off, while other configurations lead to trapping of droplets which hinder roll-off [17].

This work is a fundamental study on EW-accelerated droplet growth dynamics and condensation heat transfer. Importantly, all experiments involve condensation of humid air (with significant non-condensables) as opposed to steam condensation which has been the focus of a majority of similar studies. The influence of the voltage and frequency of the AC EW field on droplet growth and coalescence is characterized, and the underlying physics is discussed. The influence of EW fields on condensation dynamics is studied both for the pre-droplet shedding phase, and for later stages when droplets shed-off. The influence of EW fields on condensation heat transfer is estimated by measuring the condensation rate. These measurements are used in an analytical thermodynamics-based model to estimate the condensation heat transfer benefits of EW.

EXPERIMENTAL METHODS

Fabrication of condensation surface

Dropwise condensation experiments were conducted on 0.5 mm thick Indium Tin Oxide (ITO) coated glass slides. Photolithography, using a positive photoresist (AZ-5209) was used to pattern the ITO substrate. Plasma etching using CH_4 was used to etch ITO, leaving behind an interdigitated electrode layout shown in Figure 1a. The two sets of electrodes were connected to the high voltage and ground ends of a signal generator and amplifier; this generated an electric field between the two electrodes. The width of the electrode and the gap between the electrodes was 50 µm each. A 2 µm layer of CYTOP (fluoropolymer) was spin coated on the surface as the EW dielectric. CYTOP is hydrophobic, which also promotes dropwise condensation. The surface was placed on a liquid nitrogen cold plate that maintained the surface at 2±1ºC. The entire setup was located in an environmental chamber (ESPEC Platinous H-series), kept at 23±2ºC and 60±2.5% relative humidity.

Description of condensation experiments

Two types of experiments were conducted. The first involved visualization of transient droplet growth dynamics on a horizontal surface. Condensation was prevented on the cold plate (via flow of nitrogen), till the plate reached 2ºC. The EW field was then turned on for the remainder of the condensation experiment. Droplet growth was recorded with a 5X magnification lens of a Nikon Eclipse LV150N microscope. A schematic of the experimental setup is shown in Figure 1b.

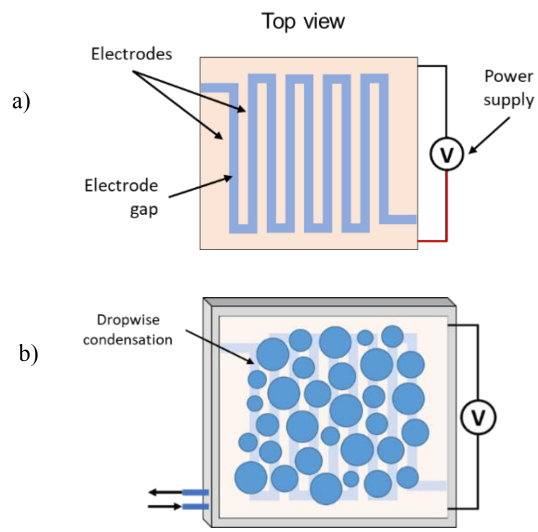

Figure 1. Schematic of experimental setup. a) Top view of condensation surface showing interdigitated electrode architecture. b) Condensing surface was placed on liquid N_2 cold plate and experiments were conducted in both horizontal and vertical orientations.

Experiments were conducted with 60 V rms and 100 V rms and at AC frequencies of 0 Hz (DC), 1 Hz and 10 kHz. Baseline experiments were also conducted in the absence of any electric field. These experiments lasted 30 minutes and capture early-stage dynamics of droplet growth and coalescence.

In the second set of experiments, the surface and setup of Figure 1b was oriented vertically and the experiments were conducted for longer durations. Droplets were seen to grow, coalesce and eventually roll-off with the rolled off droplets capturing additional condensate as they departed the surface. The condensed water was collected and measured, and is used to evaluate heat transfer. These experiments were conducted at 100 V rms and at AC frequencies of 1 Hz and 10 kHz.

Post-processing of experimental data involved the use of MATLAB to count the number and size of condensed droplets (circle finder image processing script). The software and imaging capabilities allowed the detection of droplets larger than 5 µm. Droplets were modeled assuming a spherical cap geometry, where in the absence of an EW field, the contact angle on a CYTOP surface is 120°, and EW voltage reduces the contact angle to 90°. All data reported in this manuscript is the average of three repetitions.

RESULTS

Early stage droplet growth dynamics

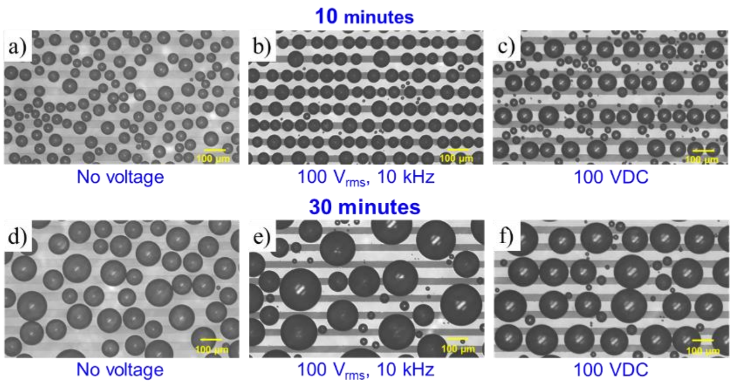

Figure 2. Droplet growth patterns under a) no voltage at 10 minutes, b) 100 Vrms, 10 kHz at 10 minutes, c) 100 VDC at 10 minutes, d) no voltage at 30 minutes, e) 100 Vrms, 10 kHz at 30 minutes, f) 100 VDC at 30 minutes.

This section highlights the influence of an EW field on droplet growth dynamics. Figure 2 shows snapshots of the surface at 10 minutes and 30 minutes for the baseline case, 100 V, 10 kHz case and 100 V DC case. In any condensation experiment nucleation, droplets initially grow by condensation of additional vapor. Coalescence occurs, once the droplets are large enough to be in contact with adjacent droplets [11]. In the absence of an EW field, droplets maintain a self-similar and homogenous random pattern even as the average droplet radius increases (Figure 2a and 2d (30 minutes)).

Under the influence of an electric field this homogenous and random distribution changes significantly. Droplets migrate to locations where the electrostatic energy of the system is minimized; this energy minima is the center of the gap between the electrodes [21,22]. Once the nucleated droplets are large enough to be affected by the electric field (for radii> 5-10µm), droplets move towards the edges of the electrodes where the field lines are concentrated. As the droplets accumulate and grow via coalescence, the field is modified by droplet (electrically conducting, compared to the insulating dielectric and air), and the minimum energy location moves to the center of the electrode gap [16]. Figure 2b shows the droplets initially aligning along these electrode gaps (dark lines) and settling in these locations. As the droplets grow, they center themselves between multiple electrode gaps as seen in Figure 2e.

Another notable aspect of the use of AC fields is the role of the AC frequency on the nature of droplet motion. At 10 kHz, the droplets migrated to the energy minimum location, but remain there, with the triple phase line oscillating about the equilibrium. However, at 1 Hz, droplets physically translated around their equilibrium position (in addition to oscillations at the triple phase line). Both types of motions, i.e. oscillation and translation are important from the viewpoint of droplet coalescence. Contact-line motion is also favorable from the point of view of reducing pinning at the triple phase-contact-line. It is noted that contact angle hysteresis and roll-off angles are lowered with AC electric fields [17].

For DC voltages, when the droplets are large enough to be affected by the electric field (i.e. hysteresis can be overcome), they move to the minimum energy location and continue to grow by further moisture condensation, or by merging of freshly nucleated droplets. Figure 2 c) and f) show droplets continuing to grow, centering themselves along the ground electrodes.

The above discussion makes it clear that electric fields will fundamentally alter droplet dynamics. Any type of externally triggered droplet motion on the condensed surface is beneficial for promoting coalescence and enhancing growth rates. To quantify the overall influence of the electric field on growth dynamics, the area-weighted average droplet radii, $< R >= \frac{\sum r^3}{\sum r^2}$ was estimated.

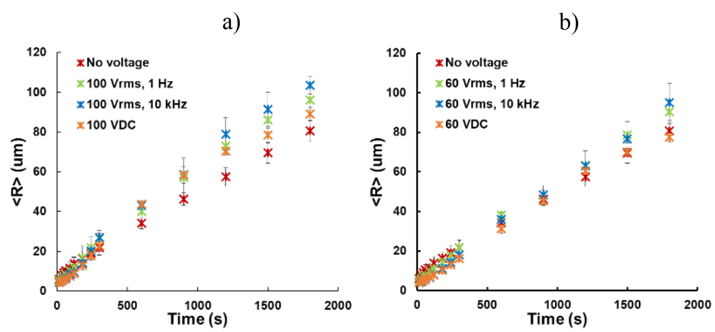

Figure 3. Area-weighted average radius of condensed droplets for a) 100 V and b) 60 V.

Figure 3 shows the evolution of $< R >$ for applied voltages of 100 V (Figure 3a) and 60 V (Figure 3b), with frequencies of 1 Hz, 10 kHz and 0 Hz (DC voltage), along with the baseline case. It is clearly seen that applying an electric field can accelerate droplet growth. Note that the differences become more pronounced at longer time scales. At the end of 30 minutes the area-weighted average droplet radius was higher than the baseline by 23% for 60 V (10 kHz) and 35% for 100 V (10 kHz). In general, faster droplet growth was observed for a 10 kHz waveform as compared to a 1 Hz waveform. This suggests that the reduced contact angle hysteresis associated with AC fields [21] makes it easier for droplets to move and coalesce. Interestingly, the DC electric field showed negligible improvements from the baseline case. For a DC field, the droplets migrated to the minimum energy position and remained there. The absence of any oscillatory motion of the contact line clearly reduces the possibility of larger droplets capturing smaller ones. Droplets can then grow only by further condensation on them or via translation of newer droplets. The nature of the electric field lines will also be different for AC versus DC fields due to the presence of droplets on the surface. For DC fields, the droplet is equipotential (no field inside the droplet), however AC fields will penetrate the droplet.

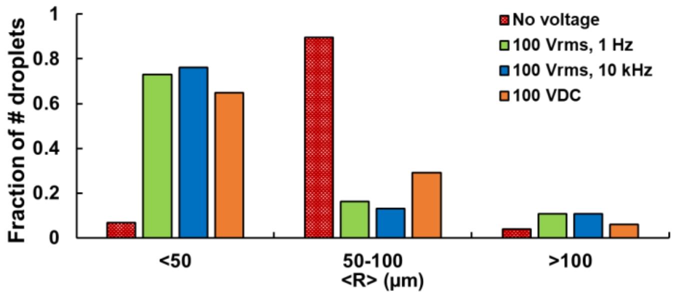

Figure 4. Distribution of droplet sizes of condensed droplets after 30 minutes under the influence of an EW voltage of 100 V.

The impact of electric fields on droplet size distributions is shown in Figure 4. For the baseline case, a unimodal log-normal distribution is observed which shows a decreasing average radius and widening distribution over time until roll-off. Under an electric field, a bi-modal or multi-modal distribution [16] is observed, where large droplets are surrounded by many small droplets. Additionally, although the distribution shows a smaller number density in the larger bin sizes under an electric field, the larger droplets account for a significantly greater volume (volume ~ r^3) percentage of the condensate. This means that under the effect of the electric field, a significant fraction of the overall condensate is captured in the larger droplets. Droplet size distribution is also important to overall enhancement of condensation heat transfer. While smaller droplets promote heat transfer (lower thermal resistance), larger droplets will sweep away significant condensate when they detach, thereby exposing fresh surfaces for nucleation. This suggests that there exists an optimum distribution that maximizes heat transfer.

Droplet roll-off and condensation rate under the influence of electric fields

This section describes the results of experiments with vertically oriented surfaces, which were run for 3 hours. Condensation rate was obtained by cumulatively summing the mass of droplets rolled-off over time. Droplet mass was estimated using image analysis to find the volume of the droplet after it had rolled down from the condensation area. Figure 5a shows the condensation mass flux for various cases. Droplet roll-off occurred when the coalesced droplets reached the critical radius for roll-off. Thereafter, the condensed mass flux was estimated using the previously described procedure. For the cases of no voltage and 100 V 10 kHz, a change in slope was seen after the initial roll-off event, where the first slope accounts for higher frequency shedding. The second region corresponds to a lower but constant slope (constant condensation rate), which is maintained for the rest of the experiment. This regime is referred to as steady state wherein droplet nucleation, growth and coalescence, and roll-off occur at various places on the surface simultaneously [9]. This is a quasi-steady process governed by a constant droplet size distribution and steady heat transfer.

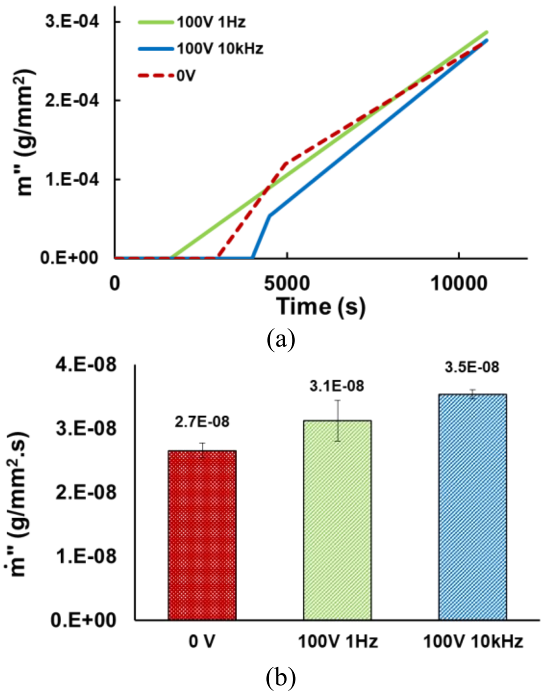

Figure 5. a) Condensed mass flux versus time for three cases (no voltage, 100 V 10 kHz, and 100 V 1 Hz), and b) Steady state condensation rate for the three cases.

Presently, the first roll-off event for the baseline case occurred at ~60 minutes. The average roll-off radius was 725±89 μm. For the case of 100 V 1 Hz, the first roll-off event occurred at ~30 minutes, and average roll-off radius was 420±100 μm. The reason for the lower roll-off radius with the electric field is the reduction in contact angle hysteresis associated with low frequency electric fields. At 100 V 10 kHz, the first roll-off events take place between 70-80 minutes with an average roll off radius of 730±75 μm. This can be attributed to the electric field pinning the droplets to the surface[17], noting that the electric field lines will penetrate the liquid at such frequencies. It is important to note that larger roll-off radii need not be detrimental to overall condensation, since the droplet size determines the volume of condensate swept.

Figure 5b shows the steady state condensation rates for the three cases. The 100 V 10 kHz case shows the highest condensation, which is 33% higher than the baseline case. This case has the largest droplet roll-off radius and the lowest frequency of droplet roll-off. The large droplets interact and capture a significant number of smaller droplets on their way down, thereby exposing new areas for fresh nucleation. For the 100 V 1 Hz case, the condensation rate is 17% higher than the baseline case. This case is characterized by low roll-off radius and high frequency of droplet roll-off events. Since the frequency of roll-off is high, there is less time for droplets to grow, and smaller droplets are swept in the path as compared to the 100 V 1 kHz case. These numbers suggest condensation can be maximized by analyzing the interactions of the large droplets with the rest of the distribution.

ANALYSIS AND DISCUSSIONS

A thermodynamics-based simplified model, which requires the total water collection rate as the input can be used to estimate and compare heat transfer. From a knowledge of the measured condensation rates the overall heat transfer rate can be estimated as:

$$Q'' = \dot{m}''h_{fg} + \dot{m}''C_{p,wv}\left(T_\infty - T_{dew\ point}\right) + h_{air}(T_\infty - T_s) \quad (1)$$

In Equation 1, the first term on the right accounts for the latent heat of condensation. The second and third terms account for sensible cooling of water vapor and air by natural convection, respectively, from ambient temperature. It is noted that a similar approach has been used to predict condensation heat transfer in atmospheric water harvesting [24].

The heat transfer coefficient of air in the natural convection term was obtained from existing heat transfer correlations [25]. h_{air} was obtained by integrating the local convection heat transfer coefficient along the length of the sample. The local heat transfer coefficient depends on the Grashof number $\left(Gr_x = \frac{g\beta(T_s - T_\infty)x^3}{\upsilon}\right)$ and the Prandtl number.

Using this model, the two cases of condensation under electric fields can be compared to the baseline case with no voltage. This analysis yields heat transfer rates of 149 W/m^2 and 157 W/m^2 for the 100 V 1 Hz and 100 V 10 kHz cases, respectively, compared to 130 W/m^2 for the no voltage case. When comparing the no voltage case, there is a 15% and 21% enhancement for the 100 V 1Hz and 100 V 10 kHz cases, respectively. It is noted that while the heat flux values are low, this study deals with condensation of humid air, and the impact of noncondensables is expected to be significant.

CONCLUSIONS

This study investigated the influence of electrowetting on dropwise condensation heat transfer enhancement on hydrophobic surfaces. It is evident that electric fields can significantly accelerate droplet coalescence and growth, and the extent of influence of the electric field depends on the nature of the field and the geometry of the electrodes. Furthermore, droplet roll-off determines condensate removal and overall heat transfer enhancement. It should be obvious that there can be several strategies for accelerating and controlling droplet growth and shedding via electric fields. Overall, this work highlights the enormous potential of electric fields in enhancing condensation heat transfer.

ACKNOWLEDGMENTS

The authors acknowledge National Science Foundation grants no. CBET-1805179 and CBET- 1653412 for supporting this work.

REFERENCES

[1] Ozkan, O., Wikramanayake, E. D., and Bahadur, V., 2017, “Modeling Humid Air Condensation in Waste Natural Gas-Powered Atmospheric Water Harvesting Systems,” Appl. Therm. Eng., 118, pp. 224–232.

[2] Kim, H., Yang, S., Rao, S. R., Narayanan, S., Kapustin, E. A., Furukawa, H., Umans, A. S., Yaghi, O. M., and Wang, E. N., 2017, “Water Harvesting from Air with Metal-Organic Frameworks Powered by Natural Sunlight.,” Science, 356(6336), pp. 430–434.

[3] Parekh, S., Farid, M. M., Selman, J. R., and Al-hallaj, S., 2004, “Solar Desalination with a Humidification-Dehumidification Technique — a Comprehensive Technical Review,” Desalination, 160(2), pp. 167–186.

[4] Paxson, A. T., Yagüe, J. L., Gleason, K. K., and Varanasi, K. K., 2014, “Stable Dropwise Condensation for Enhancing Heat Transfer via the Initiated Chemical Vapor Deposition (ICVD) of Grafted Polymer Films,” Adv. Mater., 26(3), pp. 418–423.

[5] Zhao, Y., Preston, D. J., Lu, Z., Zhang, L., Queeney, J., and Wang, E. N., 2018, “Effects of Millimetric Geometric Features on Dropwise Condensation under Different Vapor Conditions,” Int. J. Heat Mass Transf., 119, pp. 931–938.

[6] Rose, J. W., 2002, “Dropwise Condensation Theory and Experiment: A Review,” Proc. Inst. Mech. Eng. Part A J. Power Energy, 216(2), pp. 115–128.

[7] Azar, A., Bahadur, V., Kulkarni, A., Yamada, M., and Ruud, J. A., 2013, “Hydrophobic Surfaces for Control and Enhancement of Water Phase Transitions,” MRS Bull. Interfacial Mater. with Spec. Wettability, 38(5), pp. 407–411.

[8] Miljkovic, N., Enright, R., and Wang, E. N., 2012, “Effect of Droplet Morphology on Growth Dynamics and Heat Transfer during Condensation on Superhydrophobic Nanostructured Surfaces,” ACS Nano, 6(2), pp. 1776–1785.

[9] Weisensee, P. B., Wang, Y., Hongliang, Q., Schultz, D., King, W. P., and Miljkovic, N., 2017, “Condensate Droplet Size Distribution on Lubricant-Infused Surfaces,” Int. J. Heat Mass Transf., 109, pp. 187–199.

[10] Mondal, B., Mac Giolla Eain, M., Xu, Q. F., Egan, V. M., Punch, J., and Lyons, A. M., 2015, “Design and Fabrication of a Hybrid Superhydrophobic-Hydrophilic Surface That Exhibits Stable Dropwise Condensation,” ACS Appl. Mater. Interfaces, 7(42), pp. 23575–23588.

[11] Castillo, J. E., Weibel, J. A., and Garimella, S. V, 2015,

“International Journal of Heat and Mass Transfer The Effect of Relative Humidity on Dropwise Condensation Dynamics Q,” Int. J. Heat Mass Transf., 80, pp. 759–766.

[12] Birbarah, P., Li, Z., Pauls, A., and Miljkovic, N., 2015, “A Comprehensive Model of Electric-Field-Enhanced Jumping-Droplet Condensation on Superhydrophobic Surfaces,” Langmuir, 31(28), pp. 7885–7896.

[13] Yan, X., Li, J., Li, L., Huang, Z., Wang, F., and Wei, Y., 2016, “Droplet Condensation on Superhydrophobic Surfaces with Enhanced Dewetting under a Tangential AC Electric Field,” Appl. Phys. Lett., 109(16).

[14] Foulkes, T., Oh, J., Birbarah, P., Neely, J., Miljkovic, N., and Pilawa-Podgurski, R. C. N., 2017, “Active Hot Spot Cooling of GaN Transistors with Electric Field Enhanced Jumping Droplet Condensation,” Conf. Proc. - IEEE Appl. Power Electron. Conf. Expo. - APEC, pp. 912–918.

[15] Miljkovic, N., Preston, D. J., Enright, R., and Wang, E. N., 2013, “Electric-Field-Enhanced Condensation on Superhydrophobic Nanostructured Surfaces,” ACS Nano, 7(12), pp. 11043–11054.

[16] Baratian, D., Dey, R., Hoek, H., Van Den Ende, D., and Mugele, F., 2018, “Breath Figures under Electrowetting: Electrically Controlled Evolution of Drop Condensation Patterns,” Phys. Rev. Lett., 120(21), p. 214502.

[17] Dey, R., Gilbers, J., Baratian, D., Hoek, H., van den Ende, D., and Mugele, F., 2018, “Controlling Shedding Characteristics of Condensate Drops Using Electrowetting,” Appl. Phys. Lett., 113.

[18] Kim, J., and Kaviany, M., 2007, “Purging of Dropwise Condensate by Electrowetting,” J. Appl. Phys., 101(10).

[19] Kim, J., and Kaviany, M., 2010, “Electrowetting Purged Surface Condensate in Evaporators,” Heat Transf. Eng., 31(2), pp. 101–107.

[20] Yan, R., McClure, T. S., Jasim, I. H., Koppula, A. K. R., Wang, S., Almasri, M., and Chen, C.-L., 2018, “Enhanced Water Capture Induced with Electrowetting-on-Dielectric (EWOD) Approach,” Appl. Phys. Lett., 113(20), p. 204101.

[21] Mugele, F., and Baret, J.-C., 2005, “Electrowetting: From Basics to Applications,” J. Phys. Condens. Matter, 17(28), pp. R705–R774.

[22] Bahadur, V., and Garimella, S. V., 2006, “An Energy-Based Model for Electrowetting-Induced Droplet Actuation,” J. Micromechanics Microengineering, 6, pp. 1494–1503.

[23] Watanabe, N., Aritomi, M., and Machida, A., 2014, “Time-Series Characteristics and Geometric Structures of Drop-Size Distribution Density in Dropwise Condensation,” Int. J. Heat Mass Transf., 76, pp. 467–483.

[24] Wikramanayake, E. D., and Bahadur, V., 2016, “Flared Natural Gas-Based Onsite Atmospheric Water Harvesting (AWH) for Oilfield Operations,” Environ. Res. Lett., 11(3), p. 034024.

[25] Incropera, F. P., DeWitt, D. P., Bergman, T. L., and Lavine, A. S., 2006, “Fundamentals of Heat and Mass Transfer,” *6th Edition*, WILEY.